

# DIRECT DETECTION OF EXTRA-SOLAR COMETS IS POSSIBLE

M. Jura

*Department of Physics and Astronomy, University of California, Los Angeles CA  
90095-1562; jura@clotho.astro.ucla.edu*

## ABSTRACT

The dust tails of comets similar to Hale-Bopp can scatter as much optical sunlight as does the Earth. Space-based observatories such as the Terrestrial Planet Finder or *Darwin* that will detect extra-solar terrestrial planets also will be able to detect extra-solar comets.

*Subject headings:* comets: general – planetary systems

## 1. INTRODUCTION

Bright comets have been studied for centuries and are endlessly fascinating. However, we do not know whether comets in the Solar System are typical or freakish. Here, we show that planned space missions such as TPF-C (Terrestrial Planet Finder – Coronagraph) or *Darwin* that are being designed to detect extra-solar terrestrial planets also will be able to detect extra-solar comets and thus test models for their formation and evolution.

Comets may have been indirectly detected around a variety of stars. Time-varying narrow absorption lines have been attributed to cometary tails around 12 Myr-old  $\beta$  Pic (Artymowicz 1997, Vidal-Madjar et al. 1998, Zuckerman 2001), and other young stars (Grady et al. 1996, Roberge et al. 2002). However, although Lecavelier des Etangs et al. (1996) and Li & Greenberg (1998) have proposed that much of the dust around  $\beta$  Pic arises from comets, the observed transient gas-phase absorbers contain a substantial amount of refractory material, and the degree of resemblance of these parent-bodies to ice-rich comets in the Solar System is uncertain (Karmann et al. 2001, 2003, Thebault et al. 2003).

Ensembles of comets around high-luminosity red giant stars where ice is rapidly sublimated (Stern et al. al. 1990, Ford & Neufeld 2001, Ford et al. 2004) might exist, and such a system could explain the detection of gaseous  $\text{H}_2\text{O}$  in the outflow from IRC+10216, a carbon-rich mass-losing red giant (Melnick et al. 2001). Alternatively, however, Willacy

(2004) has proposed that the observed  $\text{H}_2\text{O}$  results from catalysed reactions on the surfaces of dust grains carried in the stellar wind and does not signify a population of orbiting comets. Jura (2004) has argued that the lack of excess  $25\ \mu\text{m}$  radiation around first ascent red giants means that these stars typically have less than  $0.1\ M_\oplus$  of comet-like Kuiper Belt Objects in orbits at  $\sim 45\ \text{AU}$ .

Comets might be indirectly detected around degenerate stars. Cometary impacts can explain the presence of metals in the atmospheres of white dwarf stars which otherwise would be pure hydrogen or pure helium (Alcock et al. 1986), but this hypothesis is quite uncertain (see Zuckerman et al. 2003). Collisions of comets with neutron stars could produce  $\gamma$ -ray bursts, and upper limits to the rate of such bursts constrain the frequency of comets in orbit around neutron stars (Shull & Stern 1995).

With high-resolution ground-based optical observations, it is possible to detect individual comet gas-tails around solar-type main-sequence stars through transient absorption of the OH bands near  $3100\ \text{\AA}$ . For extra-solar environments similar to the Solar System, averaged over all possible inclinations, the chance in any randomly timed observation of detecting a large comet like Hale-Bopp by this method is only  $3 \times 10^{-8}$ , but around young stars with infrared excesses, this probability may approach 0.01 (Jura 2005).

All of these methods are somewhat indirect and are yet to provide compelling evidence for extra-solar comets. Here, we describe how comets might be directly detected because of scattering by dust in their extended tails. In particular, although the final system architecture is not developed, TPF-C is currently envisioned as a 4 by 6 m optical telescope with a coronagraph designed to find the scattered light from Earth-like planets in the habitable zone around main-sequence stars within  $\sim 15\ \text{pc}$  of the Sun. We argue that any system which will be able to obtain direct images of an analog to the Earth also will be able to detect bright comets.

## 2. DUST SCATTERING IN COMET TAILS

### 2.1. Overview

We consider only the portion of a comet’s orbit where it is close enough to its host star that there is rapid water-ice sublimation and consequently a large release of dust embedded within this ice. By integrating over the entire portion of the orbit where the comet is vigorously outgassing, we then compute the total mass of dust ejected by the comet. We show that most of the dust approximately follows the orbital trajectory of the comet’s nucleus, and we estimate the amount of light scattered by the comet’s dust tail.

We denote the water ejected by a comet between two times,  $t_1$  and  $t_2$ , as  $\Delta M_{H_2O}(t_1, t_2)$  and we set  $t = 0$  at the time of the comet’s periastron. If  $\chi_{eff}$  ( $\text{cm}^2 \text{g}^{-1}$ ) denotes the effective scattering opacity of the dust associated with the ejected water, then in the optically thin tail, the fraction,  $f_{comet}$ , of the host star’s luminosity scattered by a comet at distance  $R$  from the host star is:

$$f_{comet} \approx \frac{\chi_{eff} \Delta M_{H_2O}(t_1, t_2)}{4\pi R^2} \quad (1)$$

We apply equation (1) to an extra-solar analog to a large comet such as Hale-Bopp with a radius over 20 km and a total mass of  $\sim 3 \times 10^{19}$  g. Comets might eject  $10^{-4}$  of their total mass during a passage near the Sun (see, for example, Whipple & Huebner 1976). Thus, an analog to Hale-Bopp could release  $3 \times 10^{15}$  g. As noted in §2.2, a typical scattering opacity for dust in Solar System comets is  $\chi_{eff} = 160 \text{ cm}^2 \text{g}^{-1}$ . In this case, with  $R = 1 \text{ AU}$ , then  $f_{comet} = 1.7 \times 10^{-10}$ . Adopting 0.37 as the Earth’s albedo (Tholen et al. 2000), then even at the most favorable phase function, the fraction of the Sun’s luminosity scattered by the Earth is  $1.4 \times 10^{-10}$ . Thus, any optical facility designed to discover an analog to the Earth by its scattered light also may discover scattered light from bright comets.

## 2.2. Detailed Standard Model

We now perform a more exact evaluation of equation (1); we need to estimate both  $\chi_{eff}$  and  $\Delta M_{H_2O}(t_1, t_2)$ . We derive  $\chi_{eff}$  using data from A’Hearn et al. (1995) who observed 85 comets between 1976 and 1992 and reported  $Af\rho$  relative to the production rate by number of OH ( $\dot{N}_{OH}$ ), where  $A$  is the Bond albedo of the dust particles ejected from the comet, and where  $f$  is the fraction of the area of the projected telescope aperture of radius  $\rho$  in which the dust scatters. Introducing a constant of proportionality,  $K_0$ , we write:

$$A f \rho = K_0 \dot{N}_{OH} \quad (2)$$

Although  $K_0$  varies by more than a factor of 10 among the different comets, its average value is  $1.5 \times 10^{-26} \text{ cm s}$ .

To estimate  $\chi_{eff}$  from  $Af\rho$ , we equate two expressions for the total effective scattering area of the dust in the comet’s tail:

$$\chi_{eff} \Delta M_{H_2O}(t_1, t_2) = A f \pi \rho^2 \quad (3)$$

The time for water to reach the outer radius of the projected aperture is  $(t_2 - t_1)$  or  $\rho/v$  where  $v$  is the outflow speed of the gas from the nucleus of the comet. Therefore for observations

of comets in the Solar System where  $t_2$  is only slightly larger than  $t_1$ , we find:

$$\Delta M_{H_2O}(t_1, t_2), = \dot{N}_{H_2O} m_{H_2O} \frac{\rho}{v} \quad (4)$$

where  $m_{H_2O}$  denotes the molecular weight of water. Consequently, we can write that:

$$\chi_{eff} \dot{N}_{H_2O} = \frac{A f \rho \pi v}{m_{H_2O}} \quad (5)$$

We must also scale the OH and H<sub>2</sub>O production rates. The main OH source is the photodissociation of water (Whipple & Huebner 1976):



Given the other very uncertainties, we approximate (see Wu & Chen 1993) that water is mostly destroyed by reaction (6). Therefore

$$\dot{N}_{OH} \approx \dot{N}_{H_2O} \quad (7)$$

From equations (2) -(7), we find:

$$\chi_{eff} \approx \frac{K_0 \pi v}{m_{H_2O}} \quad (8)$$

Adopting a typical outflow speed of 1 km s<sup>-1</sup> (Whipple & Huebner 1976), then  $\chi_{eff} = 160$  cm<sup>2</sup> g<sup>-1</sup>.

For the purpose of studying extra-solar comets, we estimate the total mass of ejected water,  $\Delta M_{H_2O}(t_1, t_2)$ , in the case where  $t_2 \gg t_1$ . We only include those portions of the comet's orbit when it is warm enough that there is copious outflow of gas and dust and therefore where sublimation of water is more important than radiative cooling in determining the comet's surface temperature. In this regime, we write:

$$\dot{M}_{H_2O} \approx \frac{L_* a m_{H_2O}}{4 \pi R^2 \Delta E} \quad (9)$$

where  $a$  is the projected active area of the comet which is at distance  $R$  from the host star of luminosity  $L_*$  (Jura 2005). The energy required for the sublimation of each ice molecule,  $\Delta E$  is taken equal to  $2 \times 10^{-12}$  erg (see also Sekanina 2002). Equation (9) reproduces within a factor of 2 much more detailed models as long as the comet is closer than 2 AU to the Sun.

Using equation (9), we write:

$$\Delta M_{H_2O}(t_1, t_2) = \int_{t_1}^{t_2} \dot{M}_{H_2O} dt = \frac{L_* a m_{H_2O}}{4 \pi \Delta E} \int_{t_1}^{t_2} \frac{dt}{R^2} \quad (10)$$

We evaluate the integral in equation (10) from the usual description of cometary orbits. If  $J$  denotes the specific angular momentum of the comet, then

$$J = (R_p G M_* [1 + \epsilon])^{1/2} \quad (11)$$

where  $R_p$  is the periastron distance,  $M_*$  is the mass of the host star and  $\epsilon$  is the eccentricity of the orbit. If  $\phi$  is the angle measured from the host star between the major axis of the orbital ellipse and the position vector of the comet, then the relationship between  $\phi$  and  $t$  can be derived from:

$$J = R^2 \frac{d\phi}{dt} \quad (12)$$

Therefore, we write:

$$\frac{dt}{R^2} = \frac{d\phi}{J} \quad (13)$$

For any time,  $t$ , we can find a corresponding angle,  $\phi$ , and for any time interval,  $\Delta t$ , there is a corresponding angular spread of the orbital motion,  $\Delta\phi$ . Substituting into equation (10), and letting  $\Delta\phi_{dust}$  denote the total angle swept out by the comet from that location where  $R = 2 \text{ AU}$ , we write from equations (10) - (13):

$$\Delta M_{H_2O}(t_1, t_2) \approx \frac{L_* a m_{H_2O} \Delta\phi_{dust}}{4\pi \Delta E (R_p G M_* [1 + \epsilon])^{1/2}} \quad (14)$$

To compute  $f_{comet}$ , we assume, as assessed in §2.3, that all of the dust ejected by the comet lies within the aperture of the telescope and at the same location as the comet's nucleus. We therefore write from equations (1) and (14) that:

$$f_{comet} \approx \frac{K_0 v L_* a \Delta\phi_{dust}}{16\pi R^2 \Delta E (R_p G M_* [1 + \epsilon])^{1/2}} \quad (15)$$

For an analog to Hale-Bopp, with  $\Delta\phi_{dust} = \pi$ ,  $R_p = 0.91 \text{ AU}$ ,  $R = 1 \text{ AU}$ ,  $a = 1500 \text{ km}^2$  and  $K_0$  and  $v$  given above, we find that  $f_{comet} = 1.9 \times 10^{-10}$ , a result somewhat larger than the total amount of light scattered by the Earth. In Figure 1, we show a schematic representation of the results from equation (15), by plotting the brightness of an analog to Hale-Bopp relative to the brightness of an analog to the Earth with the assumptions that the orbits are co-planar and that we are looking at the system face-on. This figure illustrates that the comet can be brighter than the planet.

Hale-Bopp was an unusually bright comet. Because it was dynamically young, it still possessed a large amount of ice so that its “active area” from which rapid sublimation occurred was comparable to its geometric area. As comets age during subsequent passages near the Sun, they lose their volatiles and their “active areas” can become relatively small compared to their total surface area.

In Figure 1, the model comet is brighter after periastron. In contrast, observations of Solar System comets often show comparable amounts of scattered light before and after perihelion. For extra-solar comets, the amount of scattered light depends upon the total amount of ejected dust so that  $t_2 \gg t_1$ . Observations of Solar System comets are made with relatively high spatial resolution and therefore they mostly detect dust which is ejected just recently from the nucleus so that  $t_2$  is only slightly greater than  $t_1$ . In this case, according to equation (9), the rate of dust production is insensitive to whether the comet is pre- or post-periastron.

Hale-Bopp was a particularly large comet, but its perihelion of 0.91 AU was not remarkable. A smaller comet with a smaller perihelion also can produce a large amount of scattered light. To illustrate this effect, we show in Figure 2 a plot of the relative brightness of an analog to comet West with  $a = 130 \text{ km}^2$  and  $R_p = 0.20 \text{ AU}$ . We selected comet West for this purpose from the 85 comets studied by A’Hearn et al. (1995) because it both had the second smallest perihelion and one of the largest effective areas. [A’Hearn et al. did not report data for Hale-Bopp because it entered the inner Solar System after 1992, the end of their 17 year observing span.] Figure 2 shows that the amount of scattered light from an analog to comet West could be relatively large. However, unless the angular resolution of a planet-hunting telescope is particularly good, an analog to comet West may not be detected.

### 2.3. Grain Dynamics

Above, we have assumed that the grains follow the orbit of the comet’s nucleus. Because comets develop long tails as the ejected grains separate from the nucleus, we now assess this approximation.

The most important dynamical difference between a comet and its ejected dust is the outward radiation pressure on the dust. Consider  $\beta$ , the ratio of radiation pressure to gravitational force on a grain. When a spherical grain’s effective cross section equals its geometric cross section, then:

$$\beta = \frac{3 L_*}{16 \pi G M_* \rho_s r_{gr} c} \quad (16)$$

where  $r_{gr}$  ( $\mu\text{m}$ ) denotes the grain radius, and  $\rho_s$  denotes the density of the grain material. For grains with  $\rho_s = 3 \text{ g cm}^{-3}$  in orbit around a solar-type star,  $\beta = 0.19 r_{gr}^{-1}$

Radiation pressure acts like “anti-gravity” and the effective inward radial force on a grain is scaled from the true gravitational force by a factor of  $(1 - \beta)$ . In Figure 3, we plot the orbits of a comet with nearly a parabolic orbit and that of a dust particle that is ejected at periastron with  $\beta = 0.2$ . As long as the comet is within a distance of  $3R_p$  of the star,

the grains and comet lie closer than  $0.2R$ . The cometary tail is not likely to be resolved by a 5 meter telescope observing a star at  $\sim 10$  pc at  $5000 \text{ \AA}$ , and our approximation that the grains in the tail and the comet are co-located is appropriate for particles with  $\beta < 0.2$  or  $r_{gr} > 1 \text{ \mu m}$ .

We now estimate the fraction of cometary grains with  $r_{gr} \geq 1 \text{ \mu m}$ . Harker et al. (2002) have found that the grain size distribution for Hale-Bopp can be represented by the function:

$$n(r_{gr}) dr_{gr} \propto \left(1 - \frac{r_0}{r_{gr}}\right)^M \left(\frac{r_0}{r_{gr}}\right)^N \quad (17)$$

with  $r_0 = 0.1 \text{ \mu m}$ , and both  $M$  and  $N$  near 3.5. Equation (17) requires some maximum grain size for otherwise it predicts an infinite mass in the particles. However, the total cross section,  $\sigma_{tot}(r_{min})$ , is independent of this maximum size, and we write for an ensemble of grains whose minimum size is  $r_{min}$ :

$$\sigma_{tot}(r_{min}) = \int_{r_{min}}^{\infty} \pi r_{gr}^2 n(r_{gr}) dr_{gr} \quad (18)$$

We plot  $\sigma_{tot}(r_{min})/\sigma_{tot}(0.1 \text{ \mu m})$  in Figure 4 to show how the total cross section scales downward as the minimum grain size is increased. In particular, for distributions with  $r_{min} = 1 \text{ \mu m}$ , the total cross section is diminished by about a factor of 2 from the full ensemble with  $r_{min} = 0.1 \text{ \mu m}$ . Therefore, our estimate of  $f_{comet}$  given in equation (15) may be too large by this factor of 2.

### 3. EXTENSIONS OF THE STANDARD MODEL

Above, we have shown how a comet like Hale-Bopp could be detected in a “standard model”. Here, we relax some of the assumptions that we made to determine the detectability of a comet, and we consider some observational consequences of the models.

#### 3.1. Different Orbital Elements

In §2.2, we assumed that the orbit was seen face-on. Here, we note that a comet like Hale-Bopp would probably be detectable regardless of the orbital inclination. Let the comet’s motion define the  $X - Y$  plane and use standard polar coordinates to describe the position of the comet with the host star at the origin and with the definition that  $\phi = 0$  at periastron. For a comet with orbital eccentricity near 1, the position vector of the comet in the  $X - Y$

plane,  $\vec{R}$ , is:

$$\vec{R} \approx \frac{2 R_p}{1 + \cos \phi} (\hat{x} \cos \phi + \hat{y} \sin \phi) \quad (19)$$

We define the unit vector to an external observer,  $\hat{n}$ , as:

$$\hat{n} = \hat{x} \cos \theta_0 \cos \phi_0 + \hat{y} \cos \theta_0 \sin \phi_0 + \hat{z} \sin \theta_0 \quad (20)$$

As seen by this external observer, the projected distance,  $d$ , between the comet and the host star is found by

$$d = |\vec{R} \times \vec{n}| \approx \frac{2 R_p}{1 + \cos \phi} (\sin^2 \theta_0 + \cos^2 \theta_0 \sin^2(\phi - \phi_0))^{1/2} \quad (21)$$

As shown in §2.2, for an analog to Hale-Bopp, the range in values of  $\phi$  where the comet is measurably bright is approximately  $\pi$ . Therefore, regardless of  $\phi_0$ , there is always a value of  $\phi$  both where the comet is bright and where  $\sin^2(\phi - \phi_0) \approx 1$ . At this particular orbital location, we see by inspection of equation (21), that  $d \geq R_p$ . For a star at 10 pc and  $R_p = 1\text{AU}$ , this value of  $d$  corresponds to an angular separation of  $0''.1$  which equals  $5\lambda/D$  for a 5 m telescope observing at  $5000 \text{ \AA}$ . The TPF coronagraph is being designed to detect sources as faint as  $10^{-10}$  of the host star at offsets larger than  $4\lambda/D$  (see Kasdin et al. 2004). Therefore, any TPF-C system with the exquisite optics to detect a terrestrial analog at 1 AU from its host star also will be able to detect an analog to Hale-Bopp in any orbital orientation.

### 3.2. Different Kinds of Host Stars

In §2.2, we discussed the detectability of comets around stars similar to the Sun. We now consider main-sequence stars with different masses and luminosities. If a planet has a radius,  $R_{pl}$ , then the fraction of the star's light that is reflected toward us,  $f_{planet}$  is:

$$f_{planet} = \frac{\pi R_{pl}^2}{4\pi R^2} f_{sc} \quad (22)$$

where  $f_{sc}$  depends both upon the albedo of the planet and its orbital orientation and phase. Because we usually see less than the fully illuminated hemisphere of the planet, we expect that  $f_{sc}$  for an analog to the Earth typically is near 0.2. Comparing  $f_{planet}$  in equation (22) with  $f_{comet}$  in equation (15), we find:

$$\frac{f_{comet}}{f_{planet}} = \frac{K_0 v L_* a \Delta \phi_{dust}}{4\pi R_{pl}^2 \Delta E (R_p G M_* [1 + \epsilon])^{1/2} f_{sc}} \approx 2 \frac{L'_*}{(R'_p M'_*)^{1/2}} \quad (23)$$

where  $L'_*$  and  $M'_*$  are measured in solar units at  $R'_p$  is measured in AU and we used the numerical values for the different terms in equation (23) employed above. We see from



expression (23) that the possibility of detecting extra-terrestrial comets is sensitive to the luminosity of the host star. In particular, for stars with luminosities less than  $0.5 L_{\odot}$ , corresponding to spectral types later than about G8 (see Drilling & Landolt 2000), the cometary analogs to Hale-Bopp may not be any brighter than the analogs to the Earth. According to Figure 1 in Kasdin et al. (2004), about 70% of the 202 viable candidates for investigation with TPF are at least as early as G8V with  $(B-V) \leq 0.74$ . Thus, for most potential stars to be targeted with TPF-C, large comets may be as bright as an analog to the Earth.

### 3.3. Infrared Signatures

In §2.2, we have shown that an analog to comet Hale-Bopp can scatter as much optical light as can an analog to the Earth. For an object with an albedo,  $b$ , the fraction of re-radiated infrared energy compared to the amount of scattered light is  $(1 - b)/b$ . Comets usually have dust albedos lower than the Earth’s typical albedo of 0.37 (see, for example, Lisse et al. 1998, 2002). Consequently, following the arguments in §2.2, those space missions designed to detect terrestrial planets in the thermal infrared, such as TPF-I, also will be able to detect analogs to comet Hale-Bopp.

### 3.4. Optical Emission Line Signatures

In the Solar System, the gaseous outflows from comets lead to strong fluorescent emission lines. Here, we estimate the strength of the optical line emission from extra-solar comets by scaling from the optical emission spectrum of Solar System comets.

Because they are photodissociated, the molecules in the outflow from a comet have a lifetime short compared to the time the comet spends near the host star. We write  $\Delta\phi_{gas}$  to denote the angular motion of the comet as seen from the host star during the radiative lifetime of a particular gaseous molecule,  $\Delta t_{gas}$ . From equation (13), then

$$\Delta\phi_{gas} = \frac{J}{R^2} \Delta t_{gas} \quad (24)$$

We now adopt the simple approximation that in an extra-solar system comet that at a particular location in its orbit, the line to continuum ratio,  $X_{LC}$ , is given by the expression

$$X_{LC}(extra - solar) = \frac{\Delta\phi_{gas}}{\Delta\phi_{dust}} X_{LC}(Solar System) \quad (25)$$

where  $\Delta\phi_{dust}$  is described in §2.2. Implicit in this formula is the prediction that because the amount of dust contributing to the scattered continuum is relatively large, the observed line to continuum ratio in extra-solar comets is likely to be appreciably lower than in Solar System comets.

Fink & Hicks (1996) have presented a convenient set of low-resolution optical observations of Solar System comets. They report both a continuum flux at 6250 Å with a bandwidth of 36 Å and continuum-subtracted emission line strengths of C<sub>2</sub>, NH<sub>2</sub>, O I and CN in bands centered at 5520 Å, 6335 Å, 6300 Å and 9180 Å, respectively. Here, we focus on the strongest cometary emission lines which are the Swan bands of C<sub>2</sub> centered at 5520 Å. In the Solar System, the characteristic lifetime of the C<sub>2</sub> molecule at 1 AU from the Sun is about  $6 \times 10^4$  s (Fink & Hicks 1996). Consequently, for a comet in an orbit with orbital eccentricity near 1.0 with a periastron of 1AU in orbit around a 1 M<sub>☉</sub> main-sequence star, we expect from equations (11) and (24) that  $\Delta\phi_{gas} \approx 0.02$ . For  $\Delta\phi_{dust} \approx 2$ , we find from equation (25) that a representative line to continuum ratio for an extra-solar comet is diminished by a factor of 100 from the value such a comet would have during “instantaneous” observations performed within the Solar System.

In the data of Fink & Hicks (1996), there is a very large range in the observed line to continuum ratio in different comets; some objects do not exhibit any detectable emission. The comets with the three strongest line fluxes measured by Fink & Hicks (1996) were Halley, Encke and Swift-Tuttle where the ratio of the emission in the C<sub>2</sub> bands to the continuum at 6250 Å with the 36 Å bandwidth ranged from 140 to 3000, respectively. We therefore expect that bright extra-solar comets might display a line to continuum ratio in the Swan bands of between 1.4 and 30. However, only 30% of the 39 comets observed by Fink & Hicks (1996) exhibit such relatively strong C<sub>2</sub> emission; the others would have line to continuum ratios less than unity.

To detect the emission line spectrum of a comet will be demanding. For a comet that has a continuum brightness of  $2 \times 10^{-10}$  of a host star with  $m_V = 6$  mag, we find that in a bandwidth of 36 Å observed with a 5 m telescope that the photon arrival rate is  $\sim 0.006$  s<sup>-1</sup>. Therefore, in a 1 hour exposure, for a comet where the C<sub>2</sub> line to continuum flux is 5, there would be 100 line photons incident upon the telescope. With a very efficient spectrograph and detector, it may be possible to measure this flux.

## 4. DISCUSSION

We have shown that a comet like Hale-Bopp might be as bright as a terrestrial planet. We now address how frequently such bright comets might appear and how we might identify the signal as being produced by a comet.

In the Solar System, the arrival rate of comets the size of Hale-Bopp or larger is about  $7 \times 10^{-10} \text{ s}^{-1}$  (see Meech et al. 2004). The duration of its bright phase is about  $10^7 \text{ s}$ , and therefore, for the Solar System, the duty cycle when a comet like Hale-Bopp is evident is  $\sim 1\%$ . The fraction of main-sequence stars with comet clouds might be as low as 1% or even less (Shull & Stern 1995, Tremaine 1993). Alternatively, however, Heisler (1990) has argued that most new comets appear during relatively intense showers. There may be stars which possess a comet infall rate 10 times that in the Solar System, and these systems often might display a comet as bright as any analog to the Earth.

Our discussion is based on extrapolating from known comets in our own Solar System, but extra-solar comets may be quite different from ours. For example, although there is a wide range, Solar System comets have an effective dust opacity of  $160 \text{ cm}^2 \text{ g}^{-1}$ . In contrast, the typical scattering opacity of interstellar dust particles is  $\sim 10000 \text{ cm}^2 \text{ g}^{-1}$  (see, for example, Spitzer 1978, and convert from the units described in that text). This large difference in scattering efficiency results from interstellar grains being smaller and having higher albedos than cometary grains (see, for example, Lisse et al. 1998, 2004). Because the growth of comets and comet-like bodies in young stellar objects is not well understood, it is imaginable that comets 100 times brighter than Hale-Bopp might be discovered.

There are ways to distinguish between a comet and a planet. First, comets have nearly parabolic orbits while a planet’s orbit has a much smaller eccentricity. Additionally, as shown in Figures 1 and 2, we expect that the amount of light reflected by a comet is much brighter after periastron and thus the light curve of a comet is quite different from that of a planet. Finally, some comets produce distinctive broad spectral emission features produced by molecular fluorescence such as that in the  $\text{C}_2$  Swan bands. Future facilities equipped with energy-sensitive photon detectors (see Sparks & Ford 2002, Day et al. 2003) could efficiently achieve low-resolution spectroscopy and in some instances distinguish between planets and comets.

## 5. CONCLUSIONS

We find that comets as large as Hale-Bopp can scatter as much optical light as would an analog to the Earth. Future space missions such as TPF-C or *Darwin* may detect large

comets around solar-type stars. If extra-solar comets eject dust with scattering efficiencies similar to interstellar dust, then an analog to Hale-Bopp could be 100 times brighter than an analog to the Earth.

This work has been partly supported by NASA under grant NAG5-7924.

## REFERENCES

- A’Hearn, M. F., Millis, R. L., Schleicher, D. G., Osip, D. J. & Birch, P. V. 1995, *Icarus*, 118, 223
- Alcock, C., Fristrom, C. C. & Siegelman, R. 1986, *ApJ*, 302, 462
- Artymowicz, P. 1997, *Ann Rev. Earth Planet. Sci.*, 25, 175
- Day, P. K., LeDuc, H. G., Mazin, B. A., Vayonakis, A. & Zmuidzinas, J. 2003, *Nature*, 425, 817
- Drilling, J. S. & Landolt, A. U. 2000, in *Allen’s Astrophysical Quantities*, ed. A. N. Cox (New York: Springer), 381
- Fink, U. & Hicks, M. D. 1996, *ApJ*, 459, 729
- Ford, K. E. S. & Neufeld, D. A. 2001, *ApJ*, 557, L113
- Ford, K. E. S., Neufeld, D. A., Schilke, P. & Melnick, G. J. 2004, *ApJ*, 614, 990
- Grady, C. A. et al. 1996, *A&AS*, 120, 157
- Harker, D. E., Wooden, D. H., Woodward, C. E. & Lisse, C. M. 2002, *ApJ*, 580, 579
- Heisler, J. 1990, *Icarus*, 88, 104
- Jura, M. 2004, *ApJ*, 603, 729
- Jura, M. 2005, *ApJ*, 620, 487
- Karmann, C., Beust, H., & Klinger, J. 2001, *A&A*, 372, 616
- Karmann, C., Beust, H., & Klinger, J. 2003, *A&A*, 409, 347
- Kasdin, N. J. et al. 2004, *Advances in Space Research*, 34, 625
- Lecavelier Des Etangs, A., Vidal-Madjar, A. & Ferlet, R. 1996, *A&A*, 307, 542

- Li, A. & Greenberg, J. M. 1998, *A&A*, 331, 291
- Lisse, C. M., A’Hearn, M. F., Hauser, M. G., Kelsall, T., Lien, D. J., Moseley, S. H., Reach, W. T. & Silverberg, R. F. 1998, *ApJ*, 496, 971
- Lisse, C. M. et al. 2004, *Icarus*, 171, 444
- Meech, K. J., Hainaut, O. R. & Marsden, B. G. 2004, *Icarus*, 170, 463
- Melnick, G. J., Neufeld, D. A., Ford, K. E. S., Hollenbach, D. J. & Ashby, M. L. N. 2001, *Nature*, 412, 160
- Roberge, A., Feldman, P. D., Lecavelier des Etangs, A., Vidal-Madjar, A., Deleuil, M., Bouret, J.-C., Ferlet, R. & Moos, H. W. 2002, *ApJ*, 568, 343
- Sekanina, Z. 2002, *ApJ*, 566, 577
- Shull, J. M. & Stern, S. A. 1995, *AJ*, 109, 690
- Sparks, W. B. & Ford, H. C. 2002, *ApJ*, 578, 543
- Spitzer, L. 1978, *Physical Processes in the Interstellar Medium* (J. Wiley: New York)
- Stern, S. A., Shull, J. M. & Brandt, J. C. 1990, *Nature*, 345, 305
- Thebault, P., Augereau, J. C. & Beust, H. 2003, *A&A*, 408, 775
- Tholen, D. J., Tejfel, V. G. & Cox, A. N. 2000, in *Allen’s Astrophysical Quantities*, ed. A. N. Cox (New York: Springer), 293
- Tremaine, S. 1993, in *Pulsars Around Planets*, eds J. A. Phillips, J. E. Thorsen & S. R. Kulkarni, *ASP Conf Series* 36, 335
- Vidal-Madjar, A., Lecavelier des Etangs, A. & Ferlet, R. 1998, *Planet. Space Sci.*, 46, 629
- Whipple, F. L. & Huebner, W. F. 1976, *ARA&A*, 14, 143
- Willacy, K. 2004, *ApJ*, 600, L87
- Wu, C. Y. R. & Chen, F. Z. 1993, *JGR*, 98, 7415
- Zuckerman, B. 2001, *ARA&A*, 39, 549
- Zuckerman, B., Koester, D., Reid, I. N. & Hunsch, M. 2003, *ApJ*, 596, 477

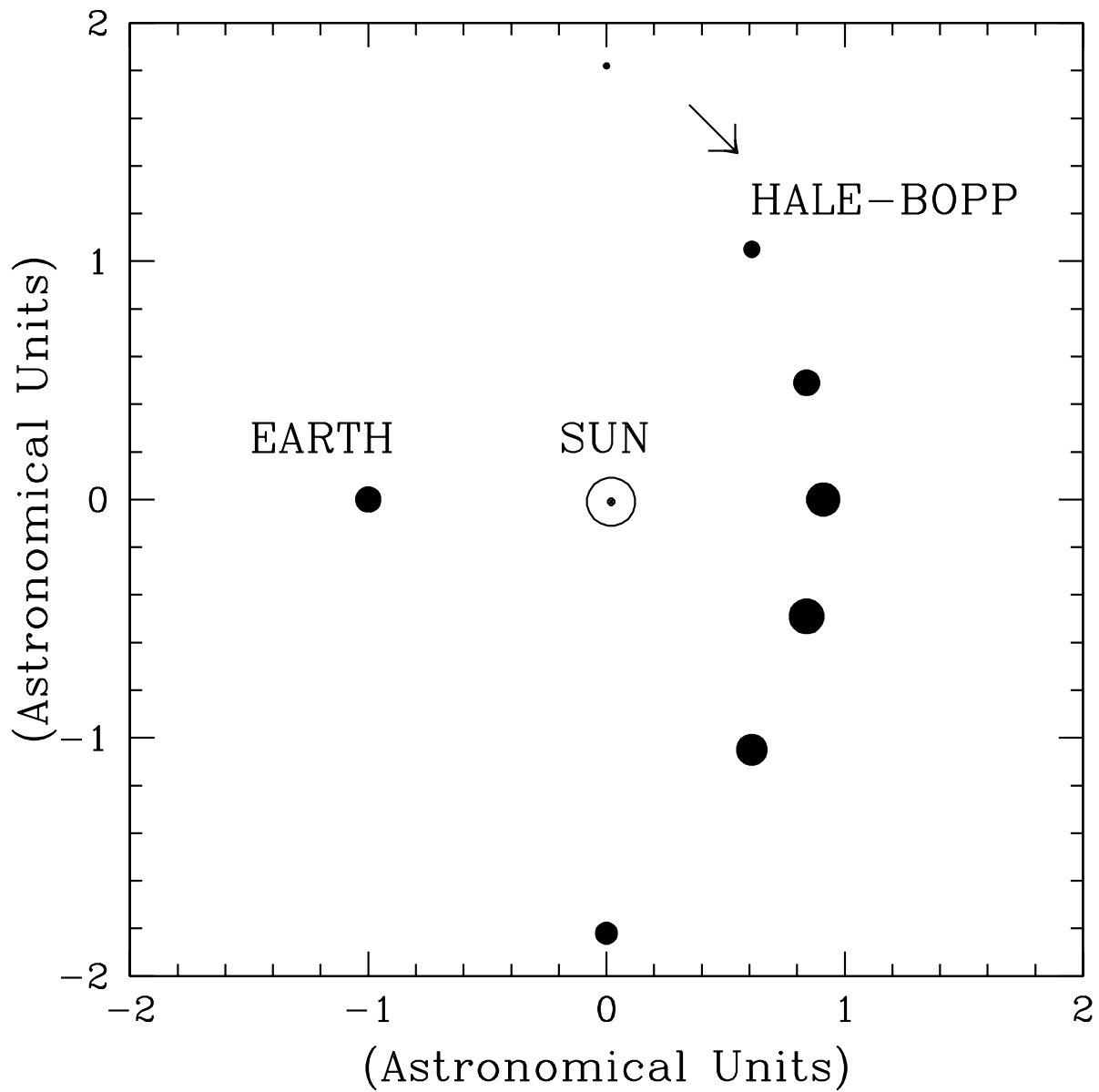


Fig. 1.— The area of each solid point scales as the optical brightness of the image of our estimate for Hale-Bopp and the Earth. We assume both the comet’s and the planet’s orbits are viewed face-on, and thus we only witness half of the illuminated hemisphere of the planet. The comet enters near the top of the diagram and exits near the bottom.

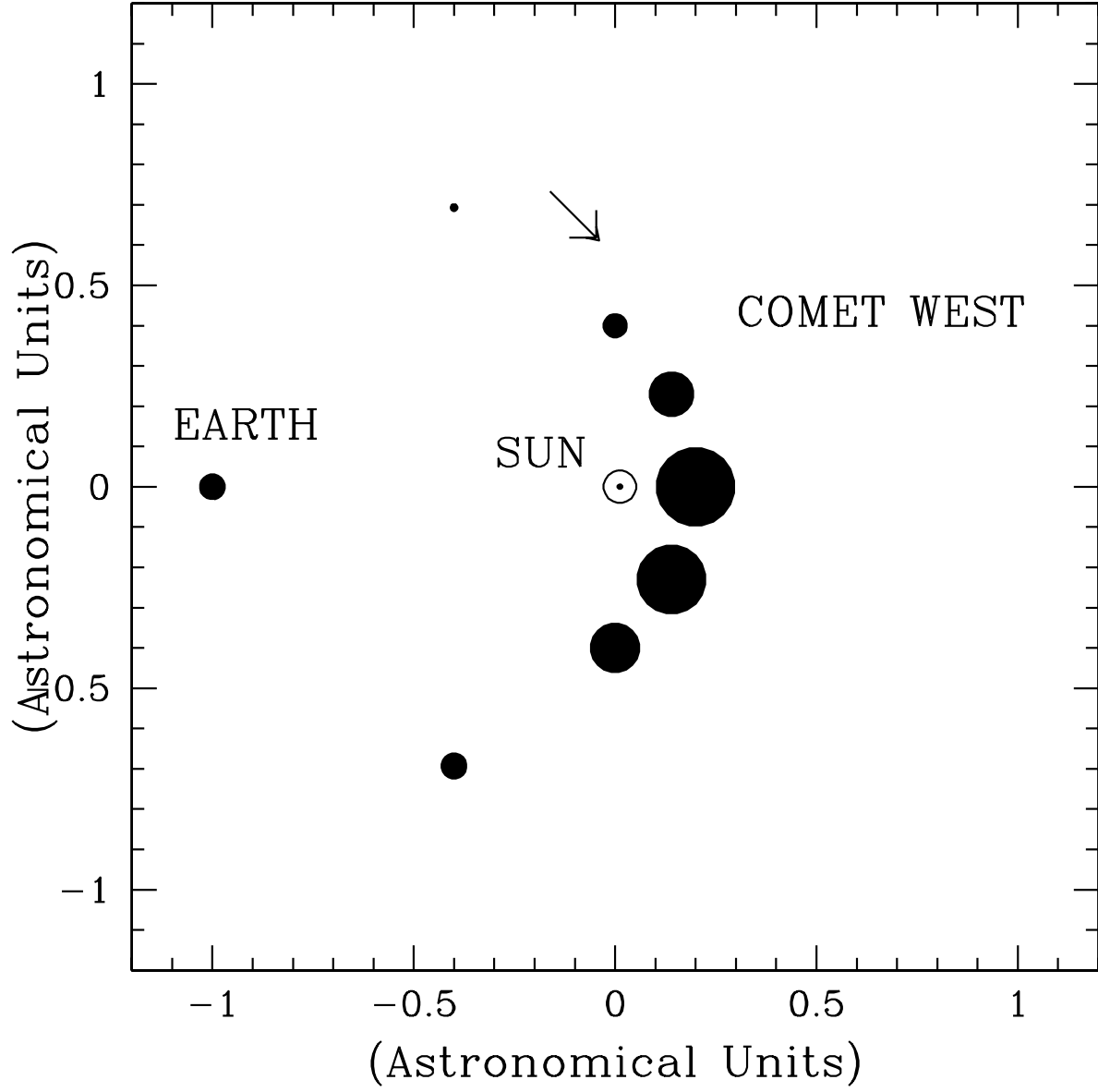


Fig. 2.— The same as Figure 1 except that we show the results for an analog of Comet West.

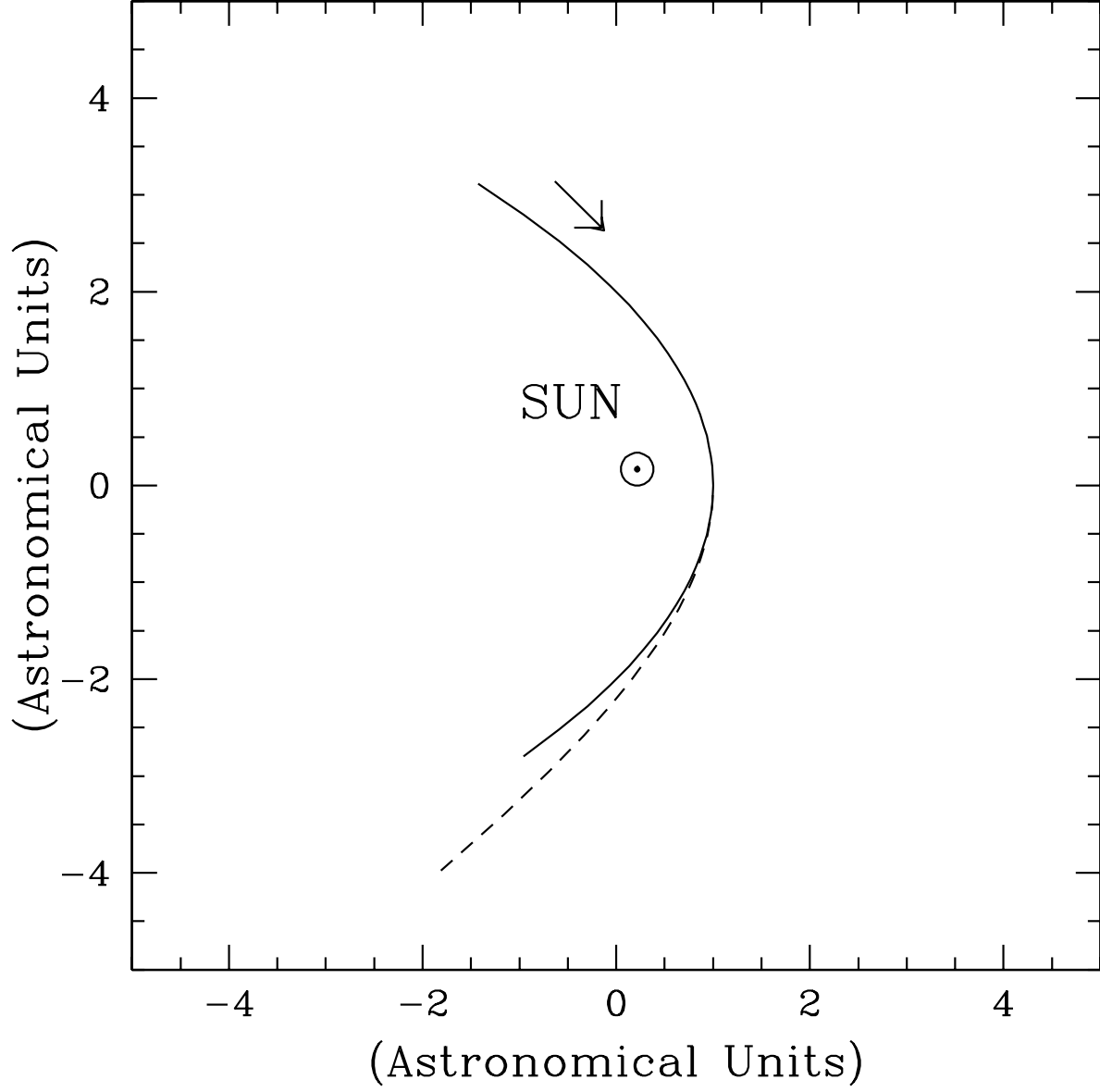


Fig. 3.— The solid line shows the inner portion of an orbit for a comet with eccentricity of 0.9999 and  $R_p = 1$  AU while the dotted line shows the orbit of a dust grain with  $\beta = 0.2$  that is ejected from the comet at perihelion. In the portions of the orbit where the comet is active, the distance between the dust grain and the comet is significantly smaller than the comet’s distance from the Sun.



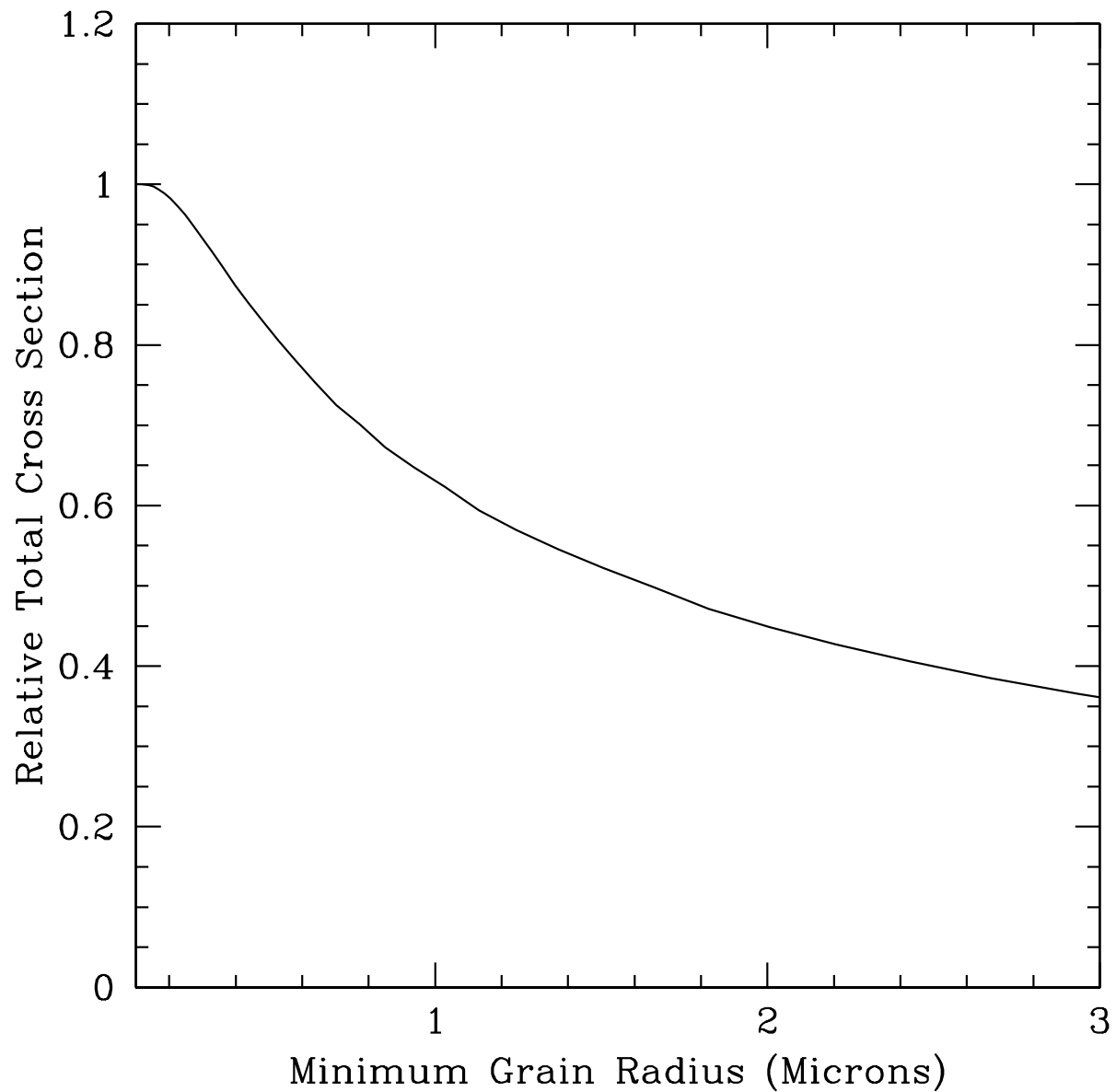


Fig. 4.— Using equations (17) and (18), we show  $\sigma_{tot}(r_{min})/\sigma_{tot}(0.1\mu m)$  vs.  $r_{min}$  to show how the integrated cross section diminishes as the minimum grain size is increased.